



Screen-printed electrode based electrochemical detector coupled with ionic liquid dispersive liquid–liquid microextraction and microvolume back-extraction for determination of mercury in water samples

Elena Fernández ^a, Lorena Vidal ^a , Daniel Martín-Yerga ^b, María del Carmen Blanco ^b, Antonio Canals ^a , Agustín Costa-García ^b

 [Show more](#)

<https://doi.org/10.1016/j.talanta.2014.11.069>

[Get rights and content](#)

This is a preprint manuscript. Please, download the final and much nicer version at:

<https://doi.org/10.1016/j.talanta.2014.11.069>

1 **Screen-Printed Electrode based Electrochemical Detector Coupled with**
2 **Ionic Liquid Dispersive Liquid-Liquid Microextraction and Microvolume**
3 **Back-Extraction for Determination of Mercury in Water Samples**

4 Elena Fernández¹, Lorena Vidal^{1*}, Daniel Martín-Yerga², María del Carmen Blanco², Antonio
5 Canals^{1*} and Agustín Costa-García²

6 ¹Departamento de Química Analítica, Nutrición y Bromatología e Instituto Universitario de
7 Materiales, Universidad de Alicante, P.O. Box 99, E-03080 Alicante, Spain.

8 ²Departamento de Química Física y Analítica, Universidad de Oviedo, C/Julián Clavería, 8,
9 33006 Oviedo, Spain.

10 *Corresponding authors: Tel.: +345909790; fax: +34965909790.

11 E-mail addresses: lorena.vidal@ua.es (L. Vidal), a.canals@ua.es (A. Canals).

12
13 **Abstract**

14 A novel approach is presented, whereby gold nanostructured screen-
15 printed carbon electrodes (SPCnAuEs) are combined with in-situ ionic liquid
16 formation dispersive liquid-liquid microextraction (in-situ IL-DLLME) and
17 microvolume back-extraction for the determination of mercury in water samples.
18 In-situ IL-DLLME is based on a simple metathesis reaction between a water-
19 miscible IL and a salt to form a water-immiscible IL into sample solution.
20 Mercury complexes with ammonium pyrrolidinedithiocarbamate (APDC) are
21 extracted from sample solution into the water-immiscible IL formed in-situ.
22 Then, an ultrasound-assisted procedure is employed to back-extract the
23 mercury into 10 μL of a HCl solution which is finally analyzed using SPCnAuEs.

24 Sample preparation methodology was optimized using a multivariate
25 optimization strategy. Under optimized conditions, a linear range between 0.5
26 and 10 $\mu\text{g L}^{-1}$ was obtained with a correlation coefficient of 0.997 for six
27 calibration points. The limit of detection obtained was 0.2 $\mu\text{g L}^{-1}$. The

28 repeatability of the proposed method was evaluated at two different spiking
29 levels (3 and 10 $\mu\text{g L}^{-1}$) and a coefficient of variation of 13% was obtained in
30 both cases. The performance of the proposed methodology was evaluated in
31 real-world water samples including tap water, bottled water and river water.
32 Relative recoveries between 97 and 107% were obtained.

33

34 **1. Introduction**

35 Mercury is one of the most well-known toxic elements and even the
36 World Health Organization places it between the first ten chemicals or group of
37 chemicals of major public health concern [1]. Mercury exists in different forms
38 with different properties, namely elemental or metallic (*i.e.* Hg^0); inorganic (*i.e.*
39 Hg^{2+}); and organic (*i.e.* MeHg^+ , EtHg^+ , PhHg^+). Several factors determine the
40 adverse effects from mercury exposure including the chemical form of mercury,
41 the dose, the age and health of the person exposed, and the duration and kind
42 of exposure (e.g. inhalation, ingestion, etc.) [2]. Among the most relevant health
43 effects we can mention damage to the gastrointestinal tract, nervous system,
44 kidneys, respiratory failures and problems during the development of organs in
45 unborn.

46 Mercury enters in the environment through both biogenic and
47 anthropogenic vias. However, human activities such as mining, burning of fossil
48 fuels, agriculture, paper and electrochemical industries, and household wastes,
49 are the main responsible of the concerning increase of mercury levels in air, soil
50 and water of certain contaminated areas. Monitoring the presence of mercury in
51 natural and drinking waters is of great interest due to its high toxicity and
52 bioaccumulation factor [3]. Mercury concentrations are commonly in the range

53 of low ng L^{-1} in environmental waters [3] whereas the permitted level of mercury
54 in drinking water depends on the responsible authorities of each territory. For
55 example, the Environmental Protection Agency (EPA) set the threshold level at
56 $2 \mu\text{g L}^{-1}$ [4] but the European Union establishes the limit at $1 \mu\text{g L}^{-1}$ [5].

57 Numerous analytical methods using capillary electrophoresis [6, 7], gas
58 [7, 8] and liquid [7, 9] chromatography, cold-vapor atomic absorption [7, 10] or
59 fluorescence [7] spectrometry, inductively coupled plasma atomic emission [7]
60 or mass spectrometry [7, 11] have been developed to determine mercury in
61 natural [7] and drinking waters [8–11]. In addition, electrochemical techniques
62 have also been widely employed and a proof of this are two excellent and
63 recently published reviews about the latest advances in electrochemical, mainly
64 voltammetric, determination of mercury [12, 13]. Electrochemistry offers
65 sensitivity, simplicity, rapid response and inexpensive instrumentation with
66 miniaturization and portable options. A major drawback to be considered results
67 from the difficulty of removing mercury from electrode surface between
68 measurements which lead to memory effect problems [12, 13]. However,
69 tedious and time consuming cleaning steps can be avoided with the use of
70 screen-printed electrodes (SPEs), which can be disposable after a single use
71 due to their high cost effectiveness. Several methods based on SPEs have
72 been reported for the determination of mercury in different water samples,
73 including the use of bare gold SPEs [14], and modified SPEs with carbon
74 nanomaterials [15–17], gold films [18, 19], gold nanoparticles [20, 21],
75 nanohybrid materials [20] and chelating agents [22, 23]. As can be seen in
76 Table 1, the vast majority of the reported works include a preconcentration step
77 over the working electrode followed by anodic stripping voltammetry. Gold is

78 commonly employed in working electrodes due to its high affinity for mercury
79 which lead to an improvement in its preconcentration. In addition, mercury
80 suffers from a process named underpotential deposition (UPD) on gold
81 electrodes [13]. The UPD process occurs by the strong interaction between the
82 two metals once the mercury is reduced forming an adsorbed layer. The
83 formation of this layer makes that UPD occurs at a more positive potential than
84 in normal conditions and, as a consequence, the selectivity of the method is
85 generally improved. In this work, screen-printed carbon electrodes (SPCEs)
86 modified with gold nanoparticles are employed as electrochemical transducers
87 in the detection stage. The use of nanoparticles in electroanalysis is
88 continuously growing due to its numerous advantages, related to the unique
89 properties of nanoparticulate materials [24] (e.g. increase surface area,
90 enhanced mass transport and improve selectivity, catalytic activity and signal to
91 noise ratio).

92 Liquid-phase microextraction (LPME) [25] appeared in the latest nineties
93 offering undoubted advantages as miniaturized extraction techniques, such as
94 simplicity, easiness to handle, low sample and solvent consumptions, and an
95 important reduction of residues generated. One of the most popular LPME
96 technique is dispersive liquid-liquid microextraction (DLLME) [26] which has
97 even come to dominate LPME research publications in the recent years [27].
98 DLLME is based on the complete dispersion of the extractant solvent into the
99 sample, normally assisted by a disperser agent. During DLLME, there is a high
100 contact between phases therefore the extraction is really rapid and effective.
101 After the extraction, phases are separated normally by centrifugation and the
102 enriched phase is analyzed. Numerous modifications of the original DLLME

103 procedure [26] have been reported up to now [28] including the use of new
104 extractant solvents such as ionic liquids (ILs) [29]. Within the use of ILs, a novel
105 methodology called in-situ IL formation dispersive liquid-liquid microextraction
106 (in-situ IL-DLLME) [30, 31] has recently been developed. In-situ IL-DLLME is
107 based on the formation of a water-immiscible IL using a metathesis reaction
108 between a water-miscible IL and an ion exchange salt into sample solution.
109 Thereby, the extractant phase is generated in-situ in form of homogeneously
110 dispersed fine drops, the disperser agent is totally avoided and the extraction
111 efficiency generally increases.

112 Different LPME techniques including single-drop microextraction [9, 32],
113 DLLME [33–35], in-situ IL-DLLME [30] and task-specific IL ultrasound-assisted
114 DLLME [36] have been employed for the determination and speciation of
115 mercury in water samples. In these works, chromatographic systems [9, 34, 35],
116 UV-Vis spectrometry [30], cold vapor [36] and electrothermal vaporization [32]
117 atomic absorption spectrometry, and capillary electrophoresis [33] were used as
118 analytical techniques.

119 The approach presented here employs an in-situ IL-DLLME followed by
120 an ultrasound-assisted microvolume back-extraction and SPCnAuEs as
121 electrochemical transducers for the determination of mercury in water samples.
122 This combination exploits the advantages of including a miniaturized sample
123 preparation step with the high sensitivity and specificity that offers the
124 electrochemical determination of mercury using SPCnAuEs. LPME provides a
125 high preconcentration of the analyte and a clean-up step for dirty matrixes
126 employing low amounts of sample and chemicals. In addition, considering the
127 low volume of sample needed for analysis with SPEs, they appear as an

128 alternative and perfectly compatible detection methodology after miniaturized
129 extraction techniques, thus avoiding classical and bulky analytical
130 instrumentation [37]. A multivariate optimization strategy has been adopted for
131 the optimization of the sample preparation and the applicability of the method
132 has been tested studying real-world water samples.

133

134 **2. Experimental part**

135 **2.1. Reagents and water samples**

136 A stock standard solution of 1000 mg L⁻¹ of Hg²⁺ was prepared by
137 dissolving Hg(OAc)₂ (≥ 99%) from Fluka (Stenheim, Germany) in ultrapure
138 water. Working solutions were prepared by proper dilution of this stock
139 standard. The IL 1-hexyl-3-methylimidazolium chloride ([Hmim][Cl]) (98%) was
140 purchased from Iolitec (Heilbronn, Germany). The lithium
141 bis[(trifluoromethyl)sulfonyl]imide (LiNTf₂) salt and the chelating agent
142 ammonium pyrrolidinedithiocarbamate (APDC) (~ 99%) were supplied by
143 Sigma-Aldrich (St. Louis, MO, USA). A solution of 2 mg mL⁻¹ of the chelating
144 agent was prepared by dissolving APDC in ultrapure water. NaCl reactive grade
145 and NaOH (≥ 97%, pellets) were from ACS Scharlau (Barcelona, Spain).
146 Fuming HCl (37%) was supplied by Merck (Madrid, Spain). The ultrapure water
147 employed for preparing all solutions was obtained with a Millipore Direct System
148 Q5TM purification system from Ibérica S.A. (Madrid, Spain).

149 Standard Au³⁺ tetrachloro complex (1.000 ± 0.002 g of AuCl₄⁻ in 500 mL
150 of 1.0 M HCl) was purchased from Merck (Madrid, Spain). Solutions of AuCl₄⁻ 1
151 mM were prepared by suitable dilution of this standard solution in HCl 0.1 M.

152 Tap water was collected from the water-supplied network of the lab in the
153 Department of Physical and Analytical Chemistry of the University of Oviedo
154 (Spain). Bottled water (San Benedetto mineral water, Valencia, Spain) was
155 purchased in the supermarket. River water from Nora river was collected in
156 Tiñana (Siero, Spain). All water samples were stored at 4 °C and were used
157 without any further pretreatment. Initial analysis confirmed that mercury levels
158 were undetectable in the three selected water samples.

159

160 **2.2. Apparatus and electrodes**

161 An ultrasonic bath from Elma (Singen, Germany) was used to assist the
162 back-extraction procedure.

163 An Autolab PGSTAT 12 potentiostat from EcoChemie (Utrecht, The
164 Netherlands) controlled by Autolab GPES software version 4.8 was used for
165 electrochemical experiments.

166 SPCEs (ref. DRP-110) with three electrode configuration were purchased
167 from DropSens (Oviedo, Spain). The working electrode, with a disk-shaped of 4
168 mm of diameter, and the counter electrode were made of a carbon ink whereas
169 the pseudo-reference electrode was made of silver. Specific connectors
170 obtained from DropSens (ref. DRP-DSC) were used for the connexion of the
171 SPCEs with the potentiostat.

172

173 **2.3. In-situ IL-DLLME and microvolume back-extraction**

174 Under optimum conditions, 20 mg of [Hmim][Cl] were placed in a test
175 tube and dissolved in 4 mL of aqueous standards or sample solutions
176 containing the analyte and the chelating agent (40 µL of 2 mg mL⁻¹). The ionic

177 exchange salt LiNTf₂ was added in an equimolar ratio (*i.e.* 28.3 mg) with the IL
178 [Hmim][Cl] and a cloudy solution was immediately formed. The mixture was
179 manually shaken for 0.5 minutes. In order to accelerate phases separation, the
180 tube was then introduced in an ice bath for 5 minutes. Next, the phases were
181 separated by centrifugation for 10 minutes at 5000 rpm. The aqueous phase
182 was removed with a glass pipette, and the formed IL-phase (*i.e.* [Hmim][NTf₂])
183 was withdrawn with a micropipette and deposited in an Eppendorf tube of 0.5
184 mL. For the back-extraction, 10 μL of HCl 4 M were added to the IL phase and
185 the mixture was sonicated in an ultrasounds bath for 14 min at 90% of power
186 and 37 KHz of frequency. After back-extraction, phases were separated by
187 centrifugation for 5 min at 5000 rpm and the enriched acidic phase that
188 remained in the upper part was analyzed.

189

190 **2.4. Electrochemical analysis**

191 Gold nanoparticles were generated over the SPCEs surface employing
192 the procedure developed by Martínez-Paredes et al. [38] and previously
193 optimized by D. Martín-Yerga et al. for the determination of mercury [20].
194 Briefly, 40 μL of a 1 mM AuCl₄⁻ solution in HCl 0.1M were dropped onto the
195 SPCE surface and a constant current of -100 μA was applied for 180 s. After
196 gold nanoparticles deposition, the electrode surface was generously rinsed with
197 ultrapure water and dried at room temperature before use. A new SPCnAuEs
198 was prepared and employed for each experiment.

199 The electrochemical behavior of mercury on SPCnAuEs was previously
200 and deeply studied [20], therefore, no further discussion will be included in the
201 present work. After back-extraction, 5 μL of the resulting upper acidic phase

202 was mixed with 37 μL of NaOH 0.5 M in order to obtain a suitable electrolytic
203 medium. A volume of 40 μL of this solution was deposited on the electrode
204 surface for the voltammetric measurements. Mercury was determined by
205 square-wave anodic stripping voltammetry (SWASV) employing previous
206 optimized conditions [20]. Mercury was preconcentrated over SPCnAuEs by
207 applying a constant potential of +0.3 V for 240 s. Thereafter, the potential was
208 recorded between +0.3 V and +0.55 V at a frequency of 80 Hz, amplitude of 30
209 mV and step potential of 4 mV. All experiments were carried out at room
210 temperature.

211

212 **2.5. Data processing**

213 An anodic peak corresponding to the reoxidation of mercury appears at
214 approximately +0.42 V and the height of this peak was employed for the
215 quantification of the analyte. The "base line correction" option provided by
216 GPEs software was employed to get more defined peaks, specially at low
217 concentrations, and to obtain more reliable and accurate measurements.

218 A two-step multivariate optimization strategy, using Plackett-Burman and
219 central composite designs, was carried out to determine the optimum conditions
220 of sample preparation. Minitab 15 statistical software (State College, PA, USA)
221 was employed to construct the experimental design matrices and evaluate the
222 results.

223

224 **3. RESULTS AND DISCUSSION**

225 **3.1. Optimization**

226 **3.1.1. Screening step**

227 Plackett-Burman design is a two-level fractional factorial design that
228 ignores interaction between variables and therefore main effects can be
229 calculated with a reduced number of experiments leading to a saving in
230 resources and time. The Plackett-Burman design results very useful in the first
231 steps of a project when many variables are initially considered but finally only a
232 few show important effects [39]. A saturated Plackett-Burman design was used
233 to construct the matrix of experiments, including 11 variables: eight real
234 variables and three dummy variables. The effects of dummy variables were
235 used to evaluate the experimental error [40, 41]. The eight real experimental
236 variables selected at two levels were: amount of [Hmim][Cl], amount of
237 chelating agent, ionic strength, pH, HCl volume, back-extraction time, power
238 and frequency of the ultrasounds bath. Table 2 shows the experimental
239 variables and levels considered in the Plackett-Burman design. A total of twelve
240 experiments were randomly performed using aqueous standards of 25 $\mu\text{g L}^{-1}$.

241 The data obtained were evaluated using an ANOVA test and the results
242 were visualized with the Pareto chart shown in Figure 1. The length of each bar
243 was proportional to the influence of the corresponding variable and the effects
244 that exceed each reference vertical line can be considered significant with a
245 95% and 90% probability, respectively.

246 According to Figure 1, the ultrasounds frequency and HCl volume were
247 statistically significant variables, with 95% probability, having a negative effect.
248 The negative effect of the frequency is in agreement with the fact that at high
249 ultrasounds frequencies, cavitation bubbles are more difficult to create as a
250 result of the shorter duration of rarefaction cycles. Higher amplitudes (*i.e.*
251 power) would be necessary to ensure that cohesive forces in the liquid were

252 overcome and maintain a certain cavitation energy [42]. For the HCl volume,
253 the negative effect is easily explained considering that if less volume of acid is
254 used, a higher concentration of the analyte is obtained. The ultrasounds device
255 employed during this work only accepted two discrete values of frequency,
256 namely 37 and 80 KHz, thus this significant variable could not be included in the
257 following optimization step and was fixed in its lower level. As a consequence,
258 back-extraction time and amount of [Hmim][Cl], which showed important effects
259 with 90% probability (see Fig. 1) were included in the optimization step. Back-
260 extraction time showed a positive effect whereas for the amount of [Hmim][Cl]
261 the effect was negative. These effects revealed that the mass transfer during
262 back-extraction is not as instantaneous as during in-situ IL-DLLME and it is
263 enhanced if low amounts of [Hmim][Cl] are used, probably because of diffusion
264 effects and the fact that a smaller volume of immiscible IL-phase is formed
265 during microextraction, and therefore a higher concentration of analyte is
266 obtained.

267 The other four real variables considered in screening step with non-
268 significant effects were fixed at the following levels: chelating agent, 40 μL (2
269 mg mL^{-1}); ionic strength, 0% of NaCl; pH, the pH of water without any
270 adjustment; and ultrasounds power, 90%.

271

272 3.1.2. Optimization of significant variables.

273 Central composite design (CCD) combines a two-level full factorial
274 design (2^k) with $2k$ star points, where k is the number of variables being
275 optimized, and one point at the center of the experimental region. In order to
276 ensure the rotatability of the model, star points were set at $\alpha = \sqrt{k} = 1.682$ whereas

277 the central point was repeated five times to provide an orthogonal design [39].
278 CCD was used to evaluate and optimize main effects, interaction effects and
279 quadratic effects of the three considered variables. Table 3 shows the low and
280 high levels, the central and star points of the considered variables in the
281 optimization step. Nineteen experiments were randomly performed using
282 aqueous standards of 25 $\mu\text{g L}^{-1}$.

283 The data obtained were also evaluated using an ANOVA test. The
284 coefficients of the variables and the p-values are listed in Table 4.

285 Significant variables with 95% probability (*i.e.* p-value < 0.05) were HCl
286 volume, back-extraction time and the quadratic effects of back-extraction time
287 and amount of [Hmim][Cl], which confirms the curvature of the system and its
288 fitting with the proposed second-grade polynomial system. The adjustment
289 obtained expressed as r^2 value was 92%.

290 The response surfaces obtained using the CCD are shown in Figure 2.
291 Pairs of variables were considered separately in order to easily interpret the
292 effect of each one on the response of the system. Thus, Figure 2a shows the
293 response surface which results of plotting HCl volume vs back-extraction time,
294 with a retention value of 40 mg for the amount of [Hmim][Cl]; Figure 2b shows
295 the response surface obtained as a function of HCl volume and amount of
296 [Hmim][Cl], whilst back-extraction time is fixed at 10 min; and Figure 2c shows
297 the surface response corresponding of the effects of back-extraction time and
298 amount of [Hmim][Cl], with established HCl volume at 40 μL . As expected, HCl
299 volume has a negative effect (Fig. 2a and b) and the response of the system
300 increases when the HCl volume decreases. For the back-extraction time, the
301 response of the system increases with the time (Fig. 2a and c) until reaching a

302 maximum at 14 min. Both, 10 μL for HCl volume and 14 min for the back-
303 extraction time, were adopted as the optimum conditions for the proposed
304 methodology. As can be seen in Fig. 2b and c, the effect of the amount of
305 [Hmim][Cl] also presents a maximum over 40 mg, although the variation of the
306 response is really slight between 40 and 20 mg. Thus, considering the sign of
307 the effect of this variable obtained in the Plackett-Burman design, which was
308 negative, and the importance of waste reduction, 20 mg of [Hmim][Cl] were
309 finally chosen for the validation of the method.

310 In summary, the results obtained from the optimization process lead to the
311 following experimental conditions: amount of [Hmim][Cl], 20 mg; chelating
312 agent, 40 μL (2 mg mL^{-1}); ionic strength, 0% of NaCl; pH, the pH of water
313 without any adjustment; HCl volume, 10 μL ; back-extraction time, 14 min;
314 ultrasounds power, 90%; and ultrasounds frequency, 37 KHz.

315

316 **3.2. Analytical figures of merit**

317 Quality parameters of the proposed method were evaluated. Under
318 optimized conditions, a concentration range from 0.5 to 25 $\mu\text{g L}^{-1}$ was studied.
319 Finally, the linear range was established between 0.5 and 10 $\mu\text{g L}^{-1}$. The
320 calibration curve was constructed using six concentration levels, evaluated by
321 triplicate. The voltammograms corresponding to the blank and the aqueous
322 standards of concentrations from 0.5 to 10 $\mu\text{g L}^{-1}$ are shown in Figure 3. The
323 resulting calibration curve gave a high level of linearity with a correlation
324 coefficient (r) of 0.997 ($N=6$). The sensitivity of the instrumental measurements
325 estimated by the slope of the calibration curve was $(3.0 \pm 0.3) \mu\text{A } \mu\text{g}^{-1} \text{ L}$. The
326 repeatability of the proposed method, expressed as coefficient of variation (CV),

327 was evaluated by five consecutive analysis of aqueous standards at
328 concentrations of 3 and 10 $\mu\text{g L}^{-1}$. CV values of 13% were found in both cases.
329 An enrichment factor of 25 was obtained for the proposed procedure, defined as
330 the slope ratio of the calibration curves with and without preconcentration.

331 The limit of detection (LOD) was estimated according to the Directive
332 98/83/EC, on the quality of water intended for human consumption, as the
333 concentration corresponding to a signal that is five times the standard deviation
334 of the blank. The LOD was found to be 0.2 $\mu\text{g L}^{-1}$, which is lower than the most
335 of the reported work up to now using SPEs (see Table 1), and stands lower
336 than the threshold value established by both, the EPA and the European Union
337 (*i.e.* 2 $\mu\text{g L}^{-1}$ and 1 $\mu\text{g L}^{-1}$, respectively). In addition, it is important to point out
338 that the sensitivity and LOD of the proposed method are significantly better than
339 those obtained in a previous work [20] (*i.e.* 0.120 $\mu\text{A } \mu\text{g}^{-1} \text{ L}$ and 3.3 $\mu\text{g L}^{-1}$,
340 respectively) using the same kind of SPCnAuEs under equal conditions but
341 without sample preparation. Therefore, the great but scarcely explored
342 advantages that offer the combination of LPME with electrochemical detection
343 using SPEs have been demonstrated.

344

345 **3.3 Real-world water samples analysis**

346 The feasibility of the proposed method to determine mercury in real-world
347 water samples was evaluated studying matrix effects. Three water samples
348 (namely tap water, bottled water and river water) were employed for recovering
349 studies. As mentioned before, previous analysis revealed that mercury levels in
350 the samples were under the LOD of the present approach. Three replicated
351 analysis of each water sample were carried out at two different spiking levels (1

352 and 7 $\mu\text{g L}^{-1}$). Relative recoveries were calculated as the ratio of the signals
353 found in real and ultrapure water samples spiked at the same concentration
354 level. As can be observed in Table 5, relative recoveries ranged from 97 to 108
355 % in the three performed water samples, whereas the CV values were between
356 9 and 15 %. According to these results, it can be concluded that the matrix
357 effects were not significant for the determination of mercury in the three
358 selected water samples.

359

360 **4. Conclusions**

361 SPCnAuEs have been successfully combined with in-situ IL-DLLME and
362 microvolume back-extraction methodologies for the determination of mercury in
363 water samples, reaching a limit of detection that satisfied the established legal
364 threshold levels and proving its application in real-world water sample analysis.

365 Higher sensitivity and lower LOD were obtained with the proposed
366 methodology compared to those obtained with the same electrochemical
367 transducers but omitting the sample preparation. Therefore, the great and up to
368 now practically unexplored benefits that offer the combination of miniaturized
369 sample preparation techniques with the electrochemical analysis using SPEs
370 have been demonstrated.

371 Although the ice-bath, centrifugation and ultrasounds limit the in-field
372 application of the proposed methodology, authors strongly believe in a
373 promising future for the combination of LPME with SPEs as detection
374 methodology within the perspectives of developing inexpensive analytical
375 methodologies with portable options for rapid and on-site measurements.

376

377

378 **Acknowledgments**

379 The authors would like to thank the Spanish Ministry of Science and Innovation
380 (project n. CTQ2011-23968), Generalitat Valenciana (Spain) (projects n.
381 ACOMP/2013/072 and PROMETEO/2013/038) and University of Alicante
382 (Spain) (project n. GRE12-45) for the financial support. E.F. also thanks
383 Generalitat Valenciana for her fellowship.

384

385 **REFERENCES**

- 386 [1] World Health Organization (2013),
387 http://www.who.int/ipcs/assessment/public_health/chemicals_phc/en/index.html.
- 388 [2] World Health Organization (2013), <http://www.who.int/mediacentre/factsheets/fs361/en/>.
- 389 [3] K. Leopold, M. Foulkes, P.J. Worsfold, *Trends Anal. Chem.*, 28 (2009) 426–435.
- 390 [4] Environmental Protection Agency (2013),
391 <http://water.epa.gov/drink/contaminants/basicinformation/mercury.cfm>.
- 392 [5] COUNCIL DIRECTIVE 98/83/EC of 3 November on the quality of water intended for human
393 consumption, .
- 394 [6] P. Kubán, P. Houserová, P. Kubán, P.C. Hauser, V. Kubán, *Electrophoresis*, 28 (2007) 58–68.
- 395 [7] K. Leopold, M. Foulkes, P. Worsfold, *Anal. Chim. Acta*, 663 (2010) 127–138.
- 396 [8] A.S. Yazdi, M.A. Ostad, F. Mofazzeli, *Chromatographia*, 76 (2013) 861–865.
- 397 [9] F. Pena-Pereira, I. Lavilla, C. Bendicho, L. Vidal, A. Canals, *Talanta*, 78 (2009) 537–541.
- 398 [10] N. Pourreza, K. Ghanemi, *J. Hazard. Mater.*, 161 (2009) 982–987.
- 399 [11] J.S. dos Santos, M. de la Guárdia, A. Pastor, M.L.P. dos Santos, *Talanta*, 80 (2009) 207–211.
- 400 [12] C. Gao, X.-J. Huang, *Trends Anal. Chem.*, 51 (2013) 1–12.
- 401 [13] D. Martín-Yerga, M.B. González-García, A. Costa-García, *Talanta*, 116 (2013) 1091–1104.
- 402 [14] E. Bernalte, C. Marín Sánchez, E. Pinilla Gil, *Anal. Chim. Acta*, 689 (2011) 60–64.
- 403 [15] F. Arduini, C. Majorani, A. Amine, D. Moscone, G. Palleschi, *Electrochim. Acta*, 56 (2011)
404 4209–4215.
- 405 [16] X. Niu, H. Zhao, M. Lan, *Anal. Sci.*, 27 (2011) 1237–1241.
- 406 [17] G. Aragay, J. Pons, A. Merkoçi, *J. Mater. Chem.*, 21 (2011) 4326–4331.
- 407 [18] A. Mandil, L. Idrissi, A. Amine, *Microchim. Acta*, 170 (2010) 299–305.
- 408 [19] S. Laschi, I. Palchetti, M. Mascini, *Sensors Actuators B Chem.*, 114 (2006) 460–465.
- 409 [20] D. Martín-Yerga, M.B. González-García, A. Costa-García, *Sensors Actuators B*, 165 (2012)
410 143–150.
- 411 [21] E. Bernalte, C.M. Sánchez, E.P. Gil, *Sensors Actuators B*, 161 (2012) 669–674.
- 412 [22] P. Ugo, L.M. Moretto, P. Bertoncello, J. Wang, *Electroanalysis*, 10 (1998) 1017–1021.

413 [23] E. Khaled, H.N.A. Hassan, I.H.I. Habib, R. Metelka, *Int. J. Electrochem. Sci.*, 5 (2010) 158–
414 167.

415 [24] F.W. Campbell, R.G. Compton, *Anal. Bioanal. Chem.*, 396 (2010) 241–259.

416 [25] F. Pena-Pereira, I. Lavilla, C. Bendicho, *Trends Anal. Chem.*, 29 (2010) 617–628.

417 [26] M. Rezaee, Y. Assadi, M.-R. Milani Hosseini, E. Aghaee, F. Ahmadi, S. Berijani, *J.*
418 *Chromatogr. A*, 1116 (2006) 1–9.

419 [27] J.M. Kokosa, *Trends Anal. Chem.*, 43 (2013) 2–13.

420 [28] H. Yan, H. Wang, *J. Chromatogr. A*, 1295 (2013) 1–15.

421 [29] M.J. Trujillo-Rodríguez, P. Rocío-Bautista, V. Pino, A.M. Afonso, *Trends Anal. Chem.*, 51
422 (2013) 87–106.

423 [30] M. Baghdadi, F. Shemirani, *Anal. Chim. Acta*, 634 (2009) 186–191.

424 [31] C. Yao, J.L. Anderson, *Anal. Bioanal. Chem.*, 395 (2009) 1491–502.

425 [32] H. Bagheri, M. Naderi, *J. Hazard. Mater.*, 165 (2009) 353–358.

426 [33] J. Li, W. Lu, J. Ma, L. Chen, *Microchim. Acta*, 175 (2011) 301–308.

427 [34] X. Jia, Y. Han, X. Liu, T. Duan, H. Chen, *Spectrochim. Acta Part B*, 66 (2011) 88–92.

428 [35] Z. Gao, X. Ma, *Anal. Chim. Acta*, 702 (2011) 50–55.

429 [36] E. Stanisz, J. Werner, H. Matusiewicz, *Microchem. J.*, 110 (2013) 28–35.

430 [37] E. Fernández, L. Vidal, J. Iniesta, J.P. Metters, C.E. Banks, A. Canals, *Anal. Bioanal. Chem.*,
431 (2013), DOI: 10.1007/s00216-013-7415-y.

432 [38] G. Martínez-Paredes, M.B. González-García, A. Costa-García, *Electrochim. Acta*, 54 (2009)
433 4801–4808.

434 [39] D.C. Montgomery, *Design and Analysis of Experiments*, 7th ed., Wiley, 2009.

435 [40] Y.V. Heyden, C. Hartmann, D.L. Massart, L. Michel, P. Kiechle, F. Erni, *Anal. Chim. Acta*, 316
436 (1995) 15–26.

437 [41] H. Fabre, N. Mesplet, *J. Chromatogr. A*, 897 (2000) 329–38.

438 [42] M.D. Priego Capote, F. Luque de Castro, *Analytical Applications of Ultrasounds*, 1st ed.,
439 Elsevier B.V., 2007.

440

441

443 **Table 1.** Comparison of different methods using SPEs for the determination of mercury in water
 444 samples.

Electrode	Lineal range	LOD	Real water samples	Comments/Analytical technique (deposition time in parentheses)	Ref.
SPGE	5-30 ng mL ⁻¹	1.1 ng mL ⁻¹	Wastewater and rain water	SWASV (60 s)	[14]
SPE/carbon black	2.5·10 ⁻⁸ -1·10 ⁻⁷ M (5-20 µg L ⁻¹)	5·10 ⁻⁹ M (1 µg L ⁻¹)	Drinking water	Indirect determination by amperometric measurements of thiols	[15]
SPBE/MWCNTs	0.2-40 µg L ⁻¹	0.09 µg L ⁻¹	Tap water	SWASV (180 s)	[16]
Carbon NP-based SPEs	1-10 µg L ⁻¹	-	Seawater	Heated electrodes/ SWASV (120 s)	[17]
SPE/gold film	2-16 µg L ⁻¹	1.5 µg L ⁻¹	Tap water	SWASV (120 s)	[18]
SPE/gold film	0.1-0.8 µg L ⁻¹	0.08 µg L ⁻¹	-	Preconcentration step using magnetic nanoparticles modified with thiols/ SWASV (120 s)	[18]
SPCE/gold film	0-100 µg L ⁻¹	0.9 µg L ⁻¹	-	SWASV (120 S)	[19]
SPGOnAuEs	2-50 µg L ⁻¹	1.9 µg L ⁻¹	-	SWASV (200 s)	[20]
SPCNTnAuEs	0.5-50 µg L ⁻¹	0.2 µg L ⁻¹	Tap and river waters	SWASV (200 s)	[20]
SPCnAuEs	5-100 µg L ⁻¹	3.3 µg L ⁻¹	-	SWASV (240 s)	[20]
SPCnAuEs	5-20 ng mL ⁻¹	0.8 ng mL ⁻¹	Rain and river waters, industrial wastewater	SWASV (120 s)	[21]
SPCE/Sumichelate a10R	-	12 pM (0.002 µg L ⁻¹)	Lagoon water	DPASV (300 s)	[22]
CTS-SPE	20-80 ng mL ⁻¹	2 ng mL ⁻¹	-	DPASV (30 s)	[23]

445 SPGE, screen-printed gold electrode; SWASV, square-wave anodic stripping voltammetry;
 446 SPBE, screen-printed bismuth electrode; MWCNTs, multi-walled carbon nanotubes; NP,
 447 nanoparticles; SPGOnAuEs, screen-printed graphene oxide/gold nanoparticles electrodes;
 448 SPCNTnAuEs, screen-printed carbon nanotubes/gold nanoparticles electrodes; DPASV,
 449 differential-pulse anodic stripping voltammetry; CTS-SPE, chitosan-modified screen-printed
 450 electrodes.

451 **Table 2.** Experimental variables and levels of the Plackett-Burman design.

Variable	Level	
	Low (-1)	High (+1)
Amount of [Hmim][Cl] (mg)	20	40
Chelating agent (μL , 2 mg mL^{-1})	20	40
Ionic strength (NaCl concentration, %, w/v)	0	10
pH	5	10
HCl volume (μL)	20	50
Back-extraction time (min)	5	10
Ultrasounds power (%)	50	90
Ultrasounds frequency (KHz)	37	80

452

453 **Table 3.** Variables and low and high levels, central and star points used in CCD design.

Variable	Level			Star points ($\alpha=1.682$)	
	Low (-1)	Central (0)	High (+1)	$-\alpha$	$+\alpha$
HCl volume (μL)	22	40	58	10	70
Back-extraction time (min)	6	10	14	3	17
Amount of [Hmim][Cl] (mg)	28	40	52	20	60

454

455

456 **Table 4.** Coefficients and p-values obtained in CCD design.

Variable	Coefficient	p-value
HCl volume (C ₁)	-15,429	0*
Back-extraction time (C ₂)	8,581	0,002*
Amount of [Hmim][Cl] (C ₃)	-3,668	0,101
C ₁ *C ₁	-0,572	0,869
C ₂ *C ₂	-13,322	0,003*
C ₃ *C ₃	-11,672	0,007*
C ₁ *C ₂	-2,863	0,533
C ₁ *C ₃	-3,429	0,458
C ₂ *C ₃	2,722	0,553

457 (*) Significant variables with 95% probability (*i.e.* p-value < 0.05).

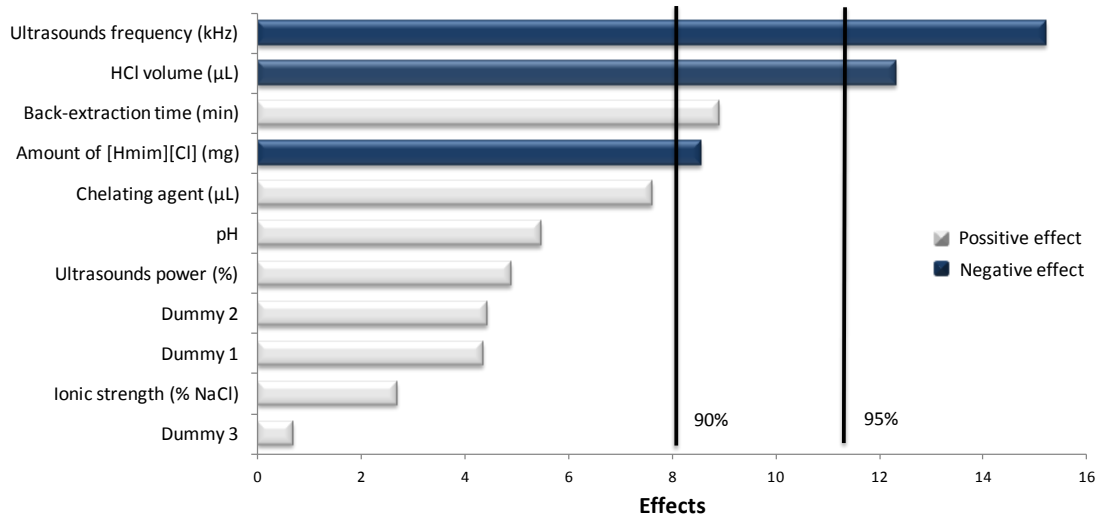
458

459 **Table 5.** Relative recoveries and CV values (in parentheses) for the analysis of mercury in real-
460 world water samples.

Water sample	Spiking level	
	1 $\mu\text{g L}^{-1}$	7 $\mu\text{g L}^{-1}$
Tap water	106 (11)	108(7)
Bottled water	98 (11)	103 (15)
River water	97 (10)	98 (9)

461

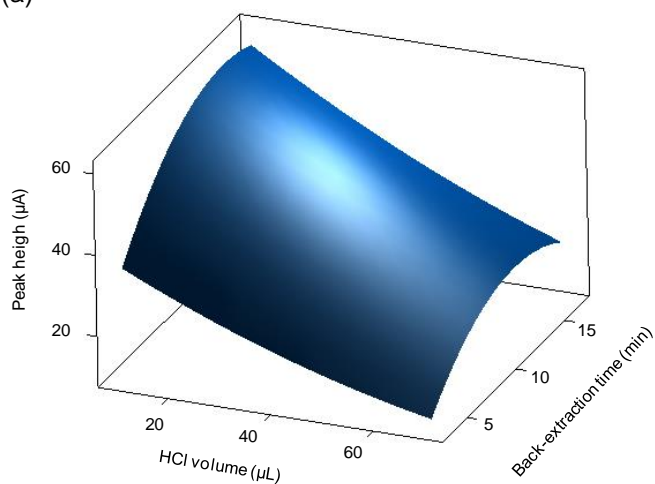
462



463

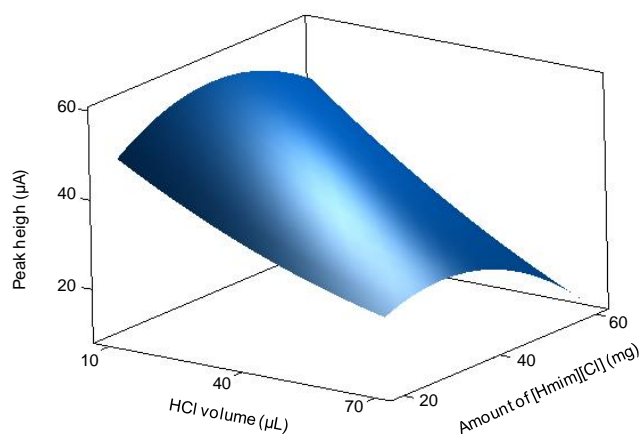
464 **Fig. 1** Pareto chart of Plackett-Burman design.

465 (a)



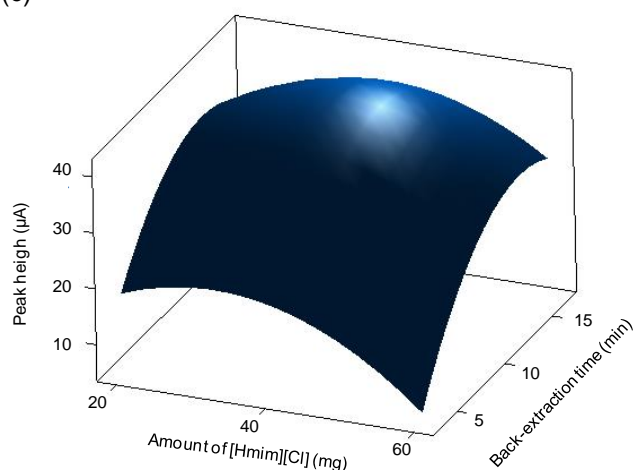
466
467
468

(b)



469
470

(c)



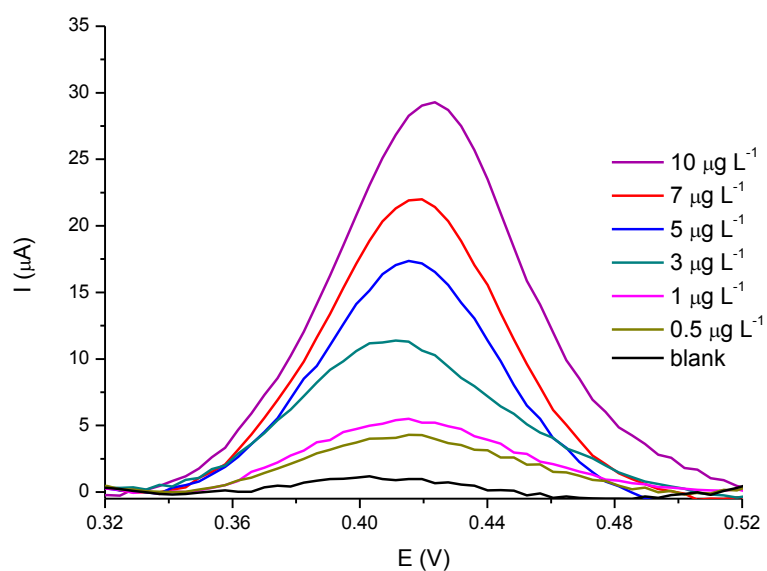
471
472
473

Fig. 2 Surface response of CCD design obtained by plotting: (a) HCl

474 volume vs. back-extraction time (amount of [Hmim][Cl]: 40 mg); (b) HCl volume

475 vs. amount of [Hmim][Cl] (back-extraction time: 10 min); (c) amount of

476 [Hmim][Cl] vs. back-extraction time (HCl volume: 40 µL).



477

478 **Fig. 3** Square-wave voltammograms, after baseline correction, of a blank and
479 mercury aqueous standards of 0.5, 1, 3, 5, 7 and 10 μg L⁻¹ after in-situ IL-
480 DLLME and back-extraction under optimum conditions.